

# Wet air oxidation in a catalytic membrane reactor: Model and industrial wastewaters in single tubes and multichannel contactors

Eduard Emil Iojoiu<sup>a</sup>, Sylvain Miachon<sup>a,\*</sup>, Emmanuel Landrивon<sup>a</sup>, John C. Walmsley<sup>b</sup>,  
Henrik Ræder<sup>b</sup>, Jean-Alain Dalmon<sup>a</sup>

<sup>a</sup> *Institut de Recherches sur la Catalyse, CNRS, 2 Av. A. Einstein, 69626 Villeurbanne, France*

<sup>b</sup> *SINTEF, P.O. Box 124 Blindern, NO-0314 Oslo, Norway*

Received 6 May 2006; received in revised form 17 June 2006; accepted 20 June 2006

Available online 4 August 2006

## Abstract

Recent results on catalytic wet air oxidation applied to a membrane contactor are presented that give new insight following a series of previous publications. Model and industrial effluents are treated in both single tube and multichannel catalytic systems. Characterisation of the catalytic material (solid analyses, electron microscopy, EDS and EPMA) is carried out, in order to determine the catalyst distribution. Catalytic results show performances heavily dependent on the nature of the effluent and the operating conditions, and to a lesser extent on the catalytic membrane characteristics. At 80 °C, an industrial effluent is oxidised at a membrane surface related rate of 3.8 mmol/s/m<sup>2</sup>. This result is achieved using a membrane containing about 0.1 wt.% Pt. This allows a revised and improved technico-economical evaluation of the *Watercatox* process.

© 2006 Elsevier B.V. All rights reserved.

**Keywords:** Catalytic wet air oxidation; Wastewater; Platinum; Membrane reactor; Multichannel system

## 1. Introduction

Wet air oxidation (WAO), developed by Zimmerman 50 years ago [1], is an attractive technology in which hazardous organics dissolved in aqueous effluents are broken down, to meet the requirements of waste reduction. Organics and inorganics are oxidized in aqueous phase under high pressure (20–200 bar air, O<sub>2</sub>, or O<sub>3</sub>) and temperature (150–350 °C) [2]. WAO is dedicated to industrial streams that are either too diluted to be efficiently treated by incineration, or are too concentrated in certain organics or salts, or contain toxic compounds, in order to be processed by biological treatment. WAO industrial plants have been mainly developed for mining and oil extraction industries [3]. The catalytic wet air oxidation (CWAO) is a further development of the WAO process using a homogenous [4] or a heterogeneous [2,3,5–10] catalyst that allows process operation under less severe reaction conditions. A recent issue of *Topics in Catalysis* was devoted to the subject [11]. However, both homogeneous and heterogeneous technologies require catalyst

recovery, and are limited by the transfer of the gaseous reactant. In order to overcome these limitations, a new system was designed, based on a catalytic membrane reactor (CMR) operated as a gas–liquid contactor [12]. CMR efficiency has been proposed in hydrogenation processes as in nitrate removal from drinking water [13], or pesticides and chlorinated hydrocarbons abatement from contaminated aqueous effluents [14]. There are further reports in the literature concerning the use of contactor CMRs in oxidation reactions applied for environmental applications [15,16].

This paper follows a series of publications [17–23] dedicated to the *Watercatox* process [24]. This process is based on a porous ceramic membrane containing catalyst nanoparticles in the top layer, acting as a gas–liquid contactor (Fig. 1). Wastewater is pumped along the contactor on the catalytic layer side, while air or oxygen flows along the other side of the contactor. The gas–liquid interface is then located within the membrane wall by means of a trans-membrane differential pressure that compensates for the gas/liquid capillary pressure.

In previous papers, it has been shown that:

- This configuration favours three-phase (gas–liquid–solid) contact, leading to a better accessibility of the reactants to the

\* Corresponding author.

E-mail address: [smiachon@catalyse.cnrs.fr](mailto:smiachon@catalyse.cnrs.fr) (S. Miachon).

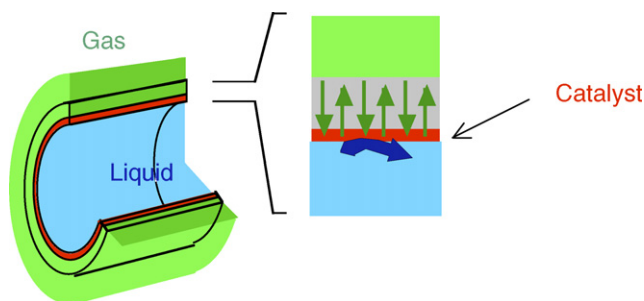


Fig. 1. Schematics of the gas–liquid catalytic interfacial contactor. The catalytic zone is in the top layer, on the tube side (dark area).

catalyst, which improves the conversion rates [18,20,25]. For example, the catalytic activity for the same catalyst (used first in membrane form, and then crushed to powder), was up to four times higher than in the conventional perfectly mixed stirred tank reactor [18,21].

- The membrane structure and properties had to be adapted to the catalytic process, while the active phase deposition had to be controlled [17,26,27]. In particular, the membrane ceramic composition was modified in order to exclude direct contact of the solution with alumina, as this oxide was proven to be involved in a slow, but irreversible, deactivation of the catalyst [18,21]. This was achieved in two cases: either the alumina-based porous membrane was covered with a nanolayer of titania, or the whole membrane structure was made of other oxides than alumina (titania, zirconia and ceria) [22,28].
- Using appropriate overpressure conditions and taking into account the specific porous structure of the membrane, the CMR operation can be optimised [20–22,25].
- The process has been successfully scaled up to a pilot unit now operating in Norway [23].

The present paper provides the most recent advances on the transition from single tubes to more realistic membrane geometries (multichannel systems), together with other practical

considerations. In particular, the issue of catalyst location within the membrane and distribution among the channels is addressed, together with their influence on catalytic performances. The influence of membrane structure, type of effluent (model and industrial) and operating conditions on the reaction rate is presented.

## 2. Experimental

### 2.1. Materials

The ceramic materials used as catalytic supports were provided by Inocermic (Germany) and Pall Exekia (France). Several characteristics regarding the structure of these asymmetric membranes are shown in Table 1.

The membranes are made of three or four concentric zones, showing an average pore size decreasing from the outside to the internal surface of the tube. The top layer is located on the inner surface of the tubes. Both endings of the membranes have been covered (ca. 1.5 cm on each side) with enamel or glaze, to give a smooth non-porous surface where viton<sup>®</sup> o-rings are allowing a tight seal.

Two different geometries of membranes have been used for this study, both sharing the structures presented in Table 1. The first experiments involved single tube membranes, especially designed and developed for lab-scale tests. For further experiments, commercial multichannel systems were used.

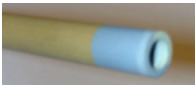



The single tubes used in this work are 10-mm external diameter, 7-mm internal diameter and 250-mm long. Multichannels supports (see Table 2 and Fig. 2) are 250-mm long. Inocermic systems, of 25-mm diameter, comprise 19 channels of 3.3-mm diameter, disposed within a cylindrical geometry, while Pall Exekia materials, of 31.5-mm diagonal, comprise 37 channels of 3-mm diameter disposed within a hexagonal geometry.

H<sub>2</sub>PtCl<sub>6</sub> (39.85% Pt, Strem Chemicals) was used as a platinum precursor to prepare the catalytic membranes. The concentration was varied according to the desired Pt loading.

Table 1  
Porous structure of the ceramic materials used in this work

Material structure	IN-4, Inocermic	PE-4, Pall Exekia	PE-3, Pall Exekia
Top layer			
Composition	CeO <sub>2</sub> /ZrO <sub>2</sub> -covered TiO <sub>2</sub>	ZrO <sub>2</sub>	ZrO <sub>2</sub>
Average pore size (nm)	~80	20	50
Thickness (μm)	≈8	≈2	≈6
First intermediate layer			
Composition	TiO <sub>2</sub>	TiO <sub>2</sub> covered α-Al <sub>2</sub> O <sub>3</sub>	–
Average pore size (μm)	0.25	0.2	
Thickness (μm)	≈27	≈14	
Second intermediate layer			
Composition	TiO <sub>2</sub>	TiO <sub>2</sub> covered α-Al <sub>2</sub> O <sub>3</sub>	TiO <sub>2</sub> covered α-Al <sub>2</sub> O <sub>3</sub>
Average pore size (μm)	0.8	0.8	0.8
Thickness (μm)	≈46	≈20	≈15
Support			
Composition	TiO <sub>2</sub>	TiO <sub>2</sub> covered α-Al <sub>2</sub> O <sub>3</sub>	TiO <sub>2</sub> covered α-Al <sub>2</sub> O <sub>3</sub>
Average pore size (μm)	5	12	12

Table 2  
Channel structure of the membranes used in this work

Inocermic	Pall Exekia
Single tube: IN-4-ST 	Single tube: PE-3-ST, PE-4-ST 
Multichannels: IN-4-MC 	Multichannels: PE-3-MC, PE-4-MC 

“IN” and “PE” refer to Inocermic and Pall Exekia materials, respectively; 3 or 4 to the number of layers; “ST” and “MC” to single tubes and multichannel systems.

Formic acid (95–98%, Riedel-de Haen) and phenol (Aldrich) were used to prepare the model solutions of 5 and 1.7 g/l, respectively, which correspond for both solutions to a total organic carbon titration (TOC) of ca. 1300 mg/l.

Three types of industrial effluents were used as wastewaters. Some of their properties are shown in Table 3. More detailed information on their composition was not accessible, due to confidentiality restriction.

## 2.2. Catalytic membrane preparation

Catalytic performance may depend on the loading and the location of platinum in the membrane. The protocol presented here is the most easily applicable to industrial scaling up. More sophisticated procedures were investigated, without providing a crucial benefit in cost to performance ratio.

In this work, catalyst deposition into the membrane support pores has been carried out using an evaporation–crystallisation technique. The samples were soaked with an  $\text{H}_2\text{PtCl}_6$  precursor solution and then dried in air in order to allow the solvent to evaporate. During the evaporation step, due to capillary forces, a progressive concentration of the platinum precursor solution towards the top layer of the channel takes place. When reaching saturation concentration, precipitation of the precursor occurs. This allowed the platinum particles to concentrate mainly into these top layers. This process has been described and modelled in previous publications from our group on single tubes [22,27].

However some precursor might be lost in the support zone by evaporation in dead-end pores. This undesired effect will depend on the texture and connectivity characteristics of the support porous structure. Impregnated membranes were calcined at 200 °C in air, in order to decompose the platinum precursor. The gas flux was then switched to hydrogen, to reduce the Pt species and form metal nanoparticles. This temperature of 200 °C is commonly used to ensure both decomposition and reduction steps.

## 2.3. Characterisation

The estimation of the total amount of platinum deposited within the structure of the membrane was based on both the mass uptake during deposition and the quantity of precursor solution absorbed within the pores during the soaking step. The results obtained through these two methods were found to be in good agreement. When related to the geometric surface area of the membranes, a surface catalytic load was obtained (in  $\text{g}_{\text{Pt}}/\text{m}^2$ ). This way of expressing the loading is preferred in the case of catalytic membranes, due to the very low weight loading used when considering the total support mass.

For multichannel systems, a more detailed estimation of the local catalyst loading was carried out using elemental chemical analysis. A special procedure of sampling precise parts of the multichannel was used. The Pt content in the top layers of the different rows of channels was obtained from the analysis of

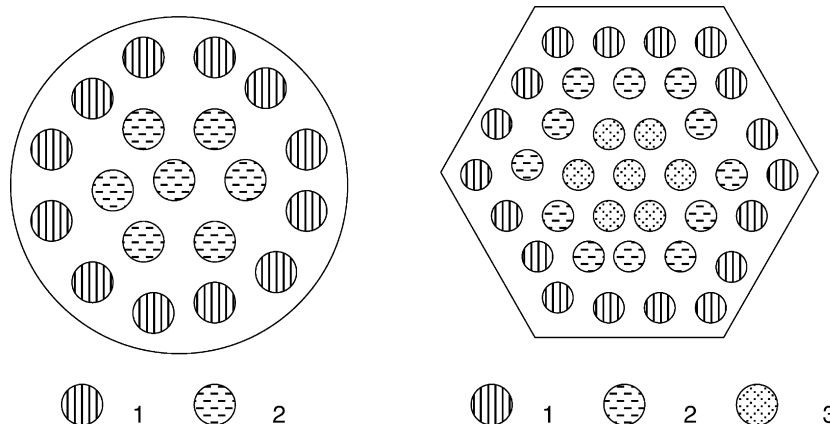


Fig. 2. Configuration of the different zones submitted to chemical analysis in the multichannel catalytic materials (Inocermic on the left and Pall Exekia on the right).

Table 3  
Composition and origin of the industrial effluents used in this study

Effluent	Wastewater type	Owner	Specific components	TOC (mg/l)
A	EOH	MONSANTO, Belgium	Formaldehyde ~0.3%; formic acid ~0.15	~1100
B	Refinery waste	DUE MILJOE, Norway	Phenolics	~6000
C	Paper industry waste		Oxalate, chlorides, sulphite, sulphates	~1300

samples collected by scratching the inner surface of the channels. The different samples were: the first row of channels (zone 1, Fig. 2), the second row of channels (zone 2), and in the case of the PE membranes, the central channels (zone 3). Moreover, the external surface of the multichannel was also analysed after local scraping, as well as the rest of the sample (referred as the bulk support).

The impregnated membranes were also characterised as well scanning electron microscopy (SEM) using a Hitachi S-4300SE field emission gun SEM and by electron probe micro-analysis (EPMA) using a JEOL JXA-8900 superprobe. Backscattered secondary electron (BSE) images were recorded in both instruments. BSE imaging is particularly useful as it is sensitive to the presence of heavy elements such as Pt. Compositions were measured by energy dispersive spectroscopy (EDS) and wavelength dispersive spectroscopy (WDS) X-ray analysis in the SEM and EPMA respectively. The samples for SEM/EPMA analysis were prepared by standard metallographic procedures, mounting in resin, grinding on silicon carbide paper, followed by a final polish using diamond paste. The samples were coated in a thin layer of carbon to eliminate charging. EMPA elementary maps were performed at  $\sim 2000\times$  magnification with an accelerating voltage of 15 kV and a step size of 0.5  $\mu\text{m}$ . Normalized Pt levels were measured for each sample.

#### 2.4. Catalytic set-up and experiments

The tubular membrane was mounted in an adapted module, using compression fittings and separating the liquid and gas feeds. For the multichannels systems, specific modules have been designed. The liquid phase was introduced in the lumen of the channel(s) and was maintained close to atmospheric pressure. The liquid feed flow rates (7 ml/min in the single tube experiments, 100 ml/min in multichannel tests, both in laminar flow) were chosen as to obtain a conversion of about 20%, in order to (i) get precise enough measurements, and (ii) avoid kinetic limitation due to an exhaust of any of the reactants. The liquid feed was kept at 1 bar absolute pressure. The gas phase was fed on the shell side under an overpressure (1–7.5 bar) monitored and carefully controlled using a pressure-difference gauge connected to a PID regulator, acting on the gas feed through a mass-flow controller. The gas feed flow rates were 50 ml/min in single tube membranes to 500 ml/min in the case of multichannel systems, keeping oxygen conversion below 25%. The membrane reactor was operated in single-pass continuous liquid flow mode. The gas overpressure steady state was reached using nitrogen, before switching to air to start the oxidation. Most experiments were carried out at 20 °C, some of them at 80 °C.

The conversion of organic compounds was monitored using a Shimadzu TOC 5050A total organic carbon analyser. The reaction rate presented in these CMR experiments is expressed as converted moles of carbon per unit time, related to the geometric membrane area, as the membrane area is the cost-limiting factor of such a process. For the purpose of comparison with conventional reactor performance, this rate can also be related to the mass of active phase.

Taking into account Laplace's law of capillary pressure, the gas–liquid interface can be shifted from the support zone toward the top layer, where the catalyst is located, by increasing the gas overpressure. For optimal control, the sealing and porous structure of the membrane and the reactor design were adapted to withstand gas overpressures up to a few atmospheres. In the present study, catalytic experiments were carried out at gas overpressures up to 10 bar.

### 3. Results

#### 3.1. Catalytic membrane characterisation

##### 3.1.1. Elemental analyses

The total platinum loading in the single tubes and multichannel membranes was found to be close to 6  $\text{g}_{\text{Pt}}/\text{m}^2$  (per unit of geometric membrane area), for high-loading membranes, and below 1  $\text{g}_{\text{Pt}}/\text{m}^2$  for low-loading membranes, as it is shown in Table 4. The calculation was based on the mass uptake after reduction and the amount of solution adsorbed in the sample during the impregnation.

For the IN-4-MC and PE-4-MC multichannel samples, as indicated in the experimental section, a more detailed assessment of platinum deposit was carried out by using elemental chemical analysis. Table 5 presents chemical analysis from different parts of their structures, for two of the multichannel systems. The zones refer to those described in Fig. 3.

Table 4  
Platinum concentration in membrane structure

Sample	$\text{g}_{\text{Pt}}/\text{m}^2$
IN-4-ST	6
IN-4-ST-low	0.2
IN-4-MC	6
IN-4-MC-low	0.9
PE-4-ST	7
PE-4-MC	5
PE-3-ST	7
PE-3-MC	5

The “-low” suffix refers to low-Pt loading samples.

Table 5  
Distribution of platinum deposit (chemical analysis basis) in IN-4-MC and PE-4-MC

Membrane	Zone	Sampling thickness ( $\mu\text{m}$ )	wt.% Pt	Pt distribution (mg)	Pt mass/channel (mg)
IN-4-MC	1 (external channel)	91	0.50	45	3.8
	2 (central channel)	61	0.23	8	1.1
	Bulk support		0.06	115	
	External surface	245	0.38	55	
	Total loading			260 <sup>a</sup>	
PE-4-MC	1 (external channel)	56	1.48	95	5.3
	2 (internal channel)	32	1.72	41	3.4
	3 (central channel)	32	1.74	25	3.5
	Bulk support		0.03	64	
	External surface	90	0.08	5	
	Total loading			378 <sup>a</sup>	

<sup>a</sup> From the precursor solution in the membrane porous volume.

The thicknesses ground from the channel walls were obtained from the mass of sample obtained. The fourth column gives the Pt weight loading of the different parts. The distribution of Pt mass between channels, bulk and external surface is shown next. The total loading was obtained from the chemical analysis of the precursor solution, assuming it was the same in the porous network of the membrane at the start of the evaporation process. This value was in good agreement

with the weight uptake of the membranes after catalyst deposition. In the case of the first membrane (IN-4-MC), the mass balance between the later and the channel, bulk and external surface chemical analyses is generally rather satisfactory. However, this is not the case of the second membrane (PE-4-MC). This sample is mainly composed of  $\alpha$ -alumina that is difficult to dissolve during chemical analysis. This could explain the inaccuracy when analysing

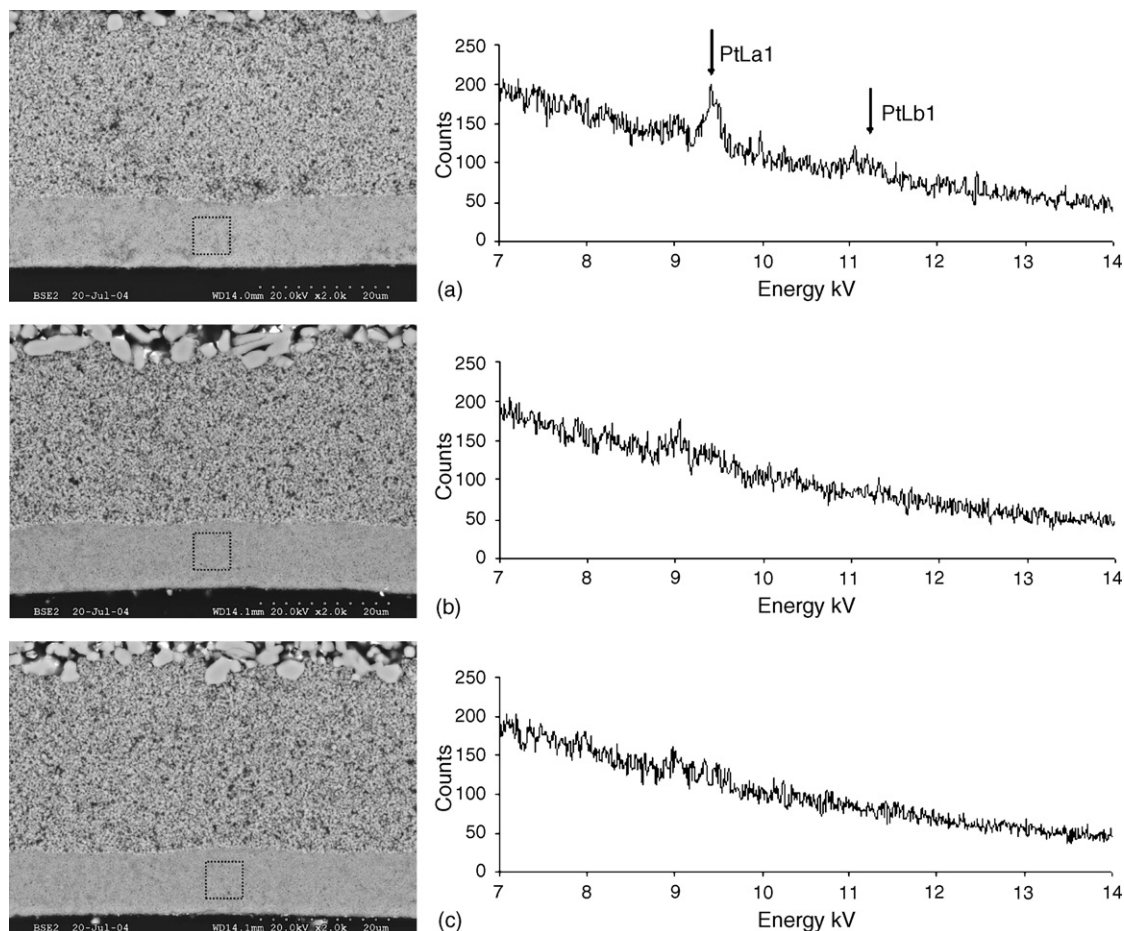


Fig. 3. SEM images showing general microstructure of top and first intermediate layers and EDS analysis of top layers for membrane IN-4-MC. (a) External channel crown, (b) intermediate channel crown and (c) central channel, showing the probe location and size on a backscattering image (left).



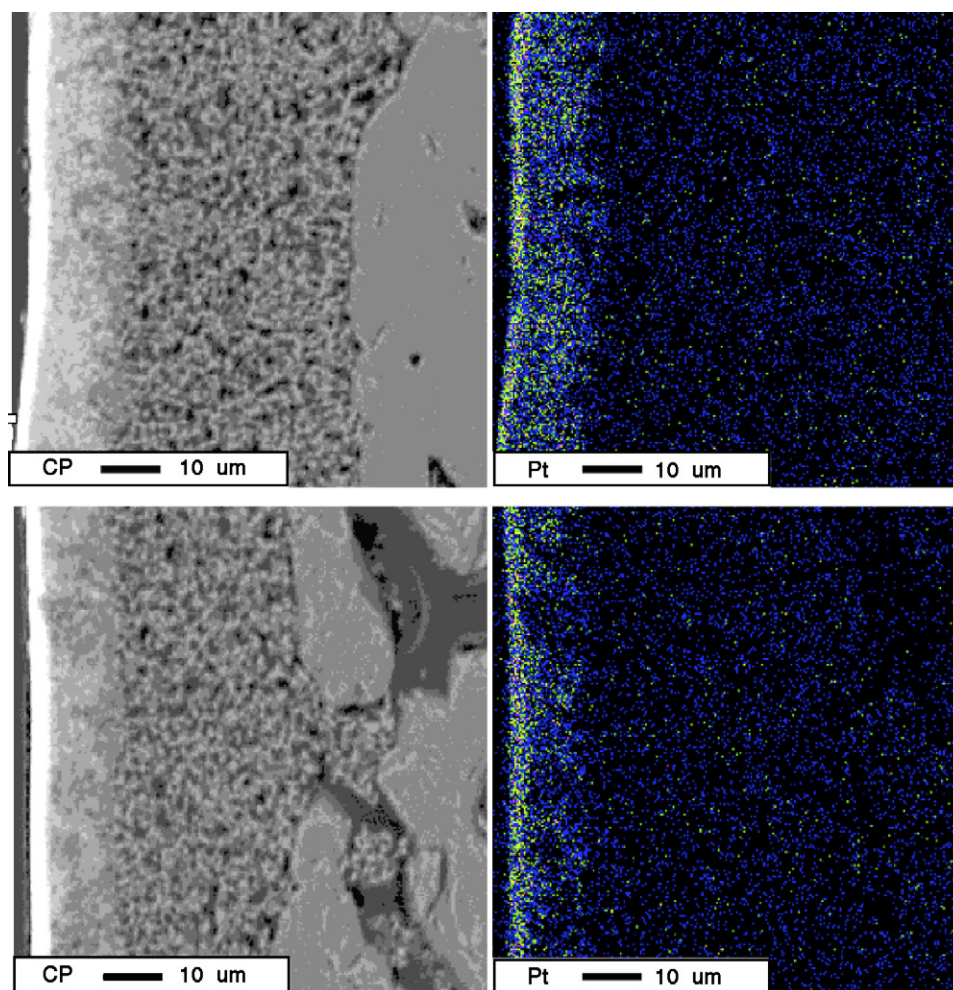


Fig. 4. Backscattering images and EPMA Pt mapping of an external (above) and central (below) channels of sample PE-4-MC.

the bulk part of the membrane, where Pt concentration is very low. The last data gives the distribution of Pt between the channels.

According to these results, the PE-4-MC membrane offers more homogeneous Pt deposition than IN-4-MC.

### 3.1.2. Electron microscopy analyses

Variations in Pt distribution between channels was also obtained by electron microscopy analyses. Heterogeneity of platinum deposition for IN-4-MC is seen in Fig. 3, which shows the microstructure and analysis obtained from external, intermediate channels and the single central channel. The BSE images show the top, first intermediate and beginning of the second intermediate layers. Contrast is uniform in the BSE images and no coarse clustering of Pt particles within the top layers was observed. EDS was performed with the electron beam scanning in a rectangular region that is indicated approximately in each top layer. The electron beam current and counting times were the same for each analysis. The energy range in the spectra including the PtL peaks, which do not overlap with peaks from other elements present in the specimen is shown in expanded detail. Pt is clearly detected in the outer channel. The signal from the intermediate channel

is extremely weak, and for the central channel no peak is detected and the Pt level has fallen below the experimental detection limit.

The amount of Pt decreases from the outer to the inner channels of the IN-4-MC sample, in keeping with chemical analyses.

EPMA analysis was also performed to map the distribution of Pt within the top and intermediate layers. Fig. 4 shows an example of this analysis performed on the PE-4-MC membrane. BSE contrast in the top layer is uniformly bright due to the presence of both Pt and Zr. There is also bright variable contrast in the first intermediate layer, that can be attributed to the distribution of Pt.

The EPMA maps show clearly that Pt is concentrated mainly in the top layer, but that some Pt, whose distribution correlates with the bright contrast in the BSE images, in the first sublayer immediately below.

EPMA profiles were also recorded on the first 25  $\mu\text{m}$  depth. Fig. 5 shows an example of these profiles, that were used to precise the Pt location. It can be seen that the Pt location follows that of the zirconia and is consistent with the EPMA mapping. The asymmetry of the profile is attributed to the longer scattering distances for the electron beam in the support resin

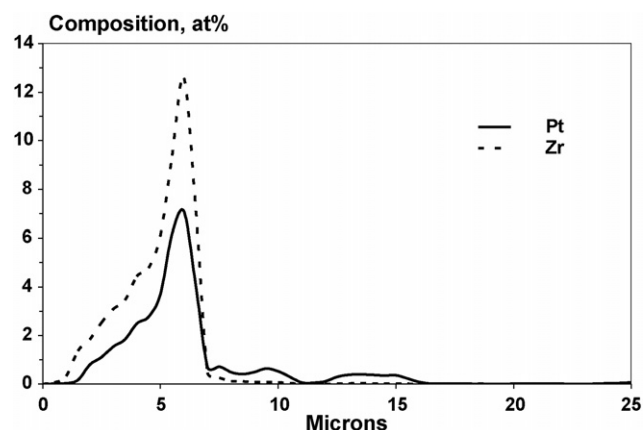


Fig. 5. EPMA Pt and Zr elemental profiles of an intermediate channel of sample PE-4-MC. The asymmetric beginning of the profile at low depth is an artefact due to enhanced scattering and spreading of the electron beam while it is still in the mounting resin close to the top layer.

used during sample preparation and the partial separation of the membrane from the resin during curing, which cause Pt and Zr signals to be generated by the electron beam while it is close to the top layer surface but still within the resin.

As far as Pt loading homogeneity among channels is concerned, these mappings suggest an even distribution, in keeping with the chemical analysis.

### 3.2. Catalytic results

#### 3.2.1. Single tubes

Reaction rates obtained on single tubes are summarised in Table 6. This table recalls data previously published on formic acid [21] and complete them with other effluents.

Using formic acid as an effluent, the maximum reaction rate was 0.9 mmol/s/m<sup>2</sup>, at 20 °C under a 5-bar air overpressure.

When phenol was used as an effluent, a reaction rate of 0.08 mmol/s/m<sup>2</sup> was obtained on IN-4-ST at 1 bar of air overpressure. Contrary to what was obtained on formic acid, increasing the air overpressure to 3.6 bars strongly decreased the reaction rate down to 0.02 mmol/s/m<sup>2</sup>. This was probably due to a deactivation phenomenon.

Industrial effluent A was rapidly oxidised, reaching a maximum rate comparable to that obtained in the case of formic acid. By contrast, wet air oxidation of the other two industrial

Table 7

Reaction rate (mmol/s/m<sup>2</sup>) on single tube membranes as a function of the type of gas and temperature

	Sample					
	IN-4-ST			PE-3-ST		
Gas at 5 bar	Air	O <sub>2</sub>	O <sub>2</sub>	Air	O <sub>2</sub>	O <sub>2</sub>
Temperature (°C)	20	20	80	20	20	80
Formic acid	0.9	1.0	2.4 <sup>a</sup>	0.9	1.0	–
Effluent A	0.5	–	–	0.9	1.3	3.8

<sup>a</sup> At 3.6 bar.

streams exhibited much lower reaction rates. On the PE-3-ST membrane, industrial effluent B, which contains a significant level of phenol, showed an initial reaction rate of 0.14 mmol/s/m<sup>2</sup>, which decreased with time.

**3.2.1.1. Single tubes: stronger experimental conditions.** In the purpose of performance evaluation, harsher conditions were applied to two effluents: model effluent (formic acid) and effluent A. These results are presented in Table 7.

Switching to pure oxygen as a gas phase in the reactor did not bring significant improvements in the reaction rate, as already noted [21]. Contrarily, increasing the temperature from 20 to 80 °C shows a clear effect.

#### 3.2.2. Multichannel membranes

The catalytic behaviour of multichannel systems obtained when formic acid was used as effluent over a wider range of pressure at 20 °C is presented in Fig. 6.

At 1 bar air overpressure, the reaction rate was almost the same (ca. 0.1 mmol/s/m<sup>2</sup>) for all three membranes. Increasing the air overpressure to 3.6 bar, the reaction rate steadily increased, reaching a maximum of 0.38–0.54 mmol/s/m<sup>2</sup>, depending on the membrane. At higher air overpressures, up to 5 bar and even 7.5 bar, only a minor increase in reaction rate was observed. It was not possible to operate the membrane PE-3-MC above 3.6 bar, due to its lower bubble point.

Among the three industrial streams (Fig. 7), the Watercatox process is more efficient for effluent A. On IN-4-MC, a maximum of 0.18 mmol/s/m<sup>2</sup> was obtained at 20 °C under 3.6 bar air overpressure. Increasing the air overpressure to 6.5 bar, the reaction rate reached 0.3 mmol/s/m<sup>2</sup>. Using effluents B or C as liquid feeds, only minor reaction rates,

Table 6

Reaction rate (mmol/s/m<sup>2</sup>) on single tube membranes as a function of air overpressure and effluent nature at 20 °C

	Sample								
	IN-4-ST			PE-4-ST			PE-3-ST		
Gas overpressure (bar)	1	3.6	5	1	3.6	5	1	3.6	5
Formic acid	0.1	0.8	0.9	0.06	0.44	0.46	0.11	0.48	0.9
Phenol	0.08	0.02	–	–	–	–	–	–	–
Effluent A	0.08	0.42	0.5	0.04	0.18	0.2	0.07	0.34	0.9
Effluent B	–	–	–	–	–	–	–	(0.14 <sup>a</sup> )	–
Effluent C	–	–	–	–	–	–	–	0.11	–

Data in italics are taken from [21].

<sup>a</sup> Deactivates.

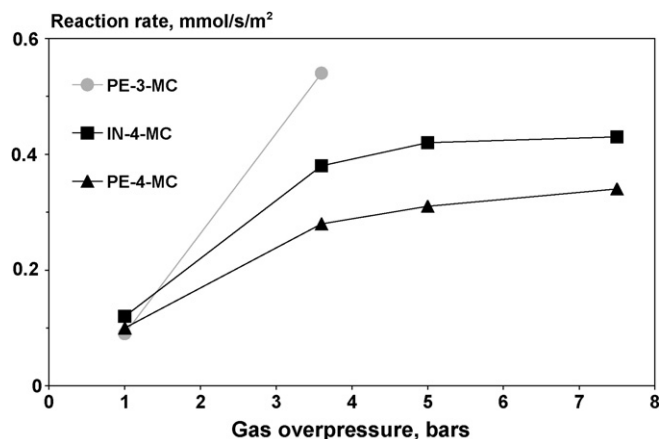


Fig. 6. Reaction rate (mmol/s/m<sup>2</sup>) as a function of gas overpressure (air) during the wet air oxidation of formic acid in an interfacial CMR at 20 °C, using Pt-impregnated multichannel membranes.

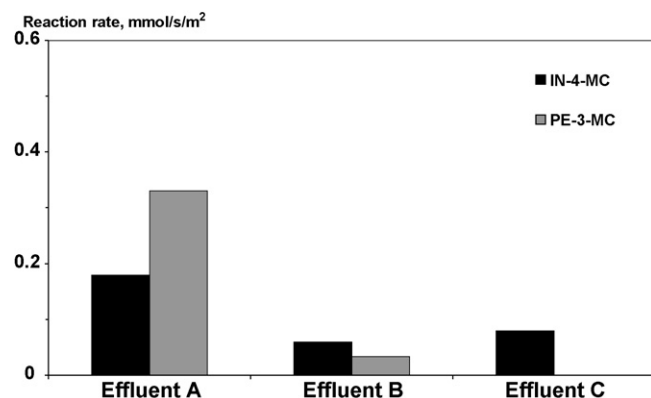


Fig. 7. Reaction rate (mmol/s/m<sup>2</sup>) as a function of effluent type, during wet air oxidation in an interfacial CMR at 20 °C under 3.6 bar of air overpressure, using Pt-impregnated multichannel membranes.

lower than 0.1 mmol/s/m<sup>2</sup> were detected. Moreover, effluent B showed rapid catalytic membrane deactivation.

### 3.2.3. Deactivation and regeneration studies on multichannel systems

It was checked that stability was not an issue for formic acid and effluent A (Fig. 8).

Taking into account that effluent C contained high levels of chlorides, as is often the case in industrial streams, the effect of chlorides on the catalyst stability has been studied. This stability assessment was performed using a formic acid solution containing a large amount of sodium chloride (20 g/l). All three membranes were tested in wet air oxidation of formic acid before and after contact with the chloride-containing solution. The results revealed a high resistance to chlorides, with no change of reaction rate being observed.

The multichannel membranes were also contacted with an effluent containing high amounts of phosphates (~10 g/l), ammonium (38 g/l), sulphates (70 mg/l) and cyanides (4 mg/l) among other components. The reaction rate of formic acid oxidation, before and after this contact, was unchanged,

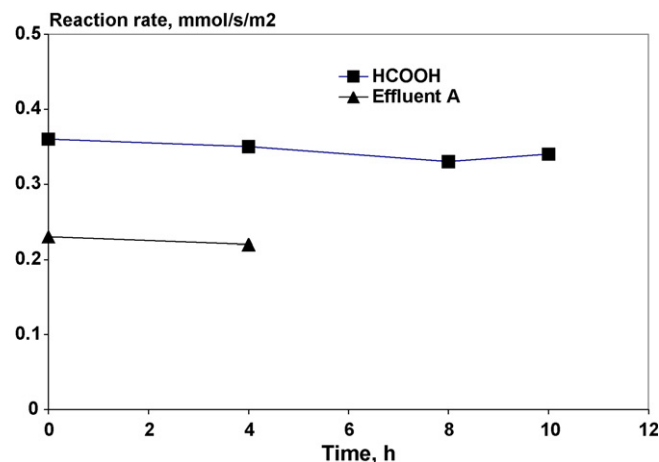


Fig. 8. Stability in time on stream of modified Pt/ceramic catalytic membrane (IN-4-MC-low) in the WAO of formic acid and effluent A at 20 °C and 7.5 bar air overpressure.

demonstrating the high stability of the catalytic membranes developed during this work.

The use of different effluents with a large variety of compositions and sometimes charged with suspended solids requires cleaning the CMR. The standard cleaning-in-place (CIP) procedure consists in back-flushing through the membrane a series of acido-basic solutions. This procedure was adapted to the laboratory conditions, dipping the membranes in the same solutions (0.5% NaOCl and 1% NaOH, 15 min at room temperature; 2% NaOH, 30 min at 70 °C; 2% HNO<sub>3</sub>, 20 min at 60 °C), in order to check their efficiency and harmlessness towards the membrane catalytic performance. For example, the same formic acid oxidation activity was obtained before and lab-CIP on a PE-4-MC membrane. Moreover, the catalytic performance was restored on fouled membranes.

Industrial application of the Watercatox process requires that no Pt is rejected in the processed stream and then to the environment. Chemical analysis of the treated effluents showed no evidence of Pt leaching.

## 4. Discussion

### 4.1. Material comparison

The main differences between the two systems are support pore size (12 and 5 μm for PE and IN samples, respectively), and channel density (5.6 and 3.9 channels/cm<sup>2</sup> section). Both electron microscopy and solid elemental analyses show that the catalyst distribution between channels is more even in the case of the PE supports. Taking into account the above differences, one can think that the evaporation within the main support zone is faster in PE tubes. The evaporation path is shorter, as the support section per channel is 37% lower, i.e. there is less solvent to evaporate for each channel (23% less). Also, as the pore size is 2.5 times larger, and the porosity is similar, the available specific surface in the support zone is about six times lower in the case of PE tubes. This leaves less surface available to lose precursor material in the support bulk during the first



phase of evaporation. As a matter of fact, some precursor is lost in the support zone, by evaporation into dead-end pores of the support zone, as was observed in single tubes. The elemental analyses clearly show that about 50% of the catalyst is deposited in the channel top layers in PE multichannels, whereas, in IN systems, this figure decreases to about 20%.

As can be seen, the two materials used here show different suitability for catalyst deposition. However, let us underline that none of them were designed for this purpose, as their usual commercial application is liquid filtration.

Concerning other samples (IN-4-MC-low and PE-3-MC), less characterisation has been performed, and no definitive conclusion has been drawn for the time being.

#### 4.2. Catalytic performance of single tubes

Let us underline these tests were carried out in order to precise the optimal porous structure and operating conditions for the multichannel systems. Effluent A shows similar transmembrane air overpressure influence on the reaction rate to that previously published on formic acid [21]. Let us recall that this was not attributed to a kinetic effect of the oxygen partial pressure, as can be seen in Table 7, but rather to the gas/liquid interface shift within the membrane porous network [20,21,25,29,30]. This interface shift is more easily evidenced when comparing the pressure increase from 3.6 to 5 bar on three- and four-layer PE structures. At 5 bar overpressure, the gas–liquid interface is closer to the catalytic zone in the three-layer structure, leading to higher catalytic performance. This is true for both effluent A and formic acid. However, it should be emphasised that the composition of effluent A (twice as much formaldehyde than formic acid), has an influence on the kinetics, depending on the membrane structure. In most cases, effluent A shows half the catalytic activity of pure formic acid, except at higher pressures on membrane PE-3-ST, when the interface is closer to the top layer. At this stage the activity is similar for both effluents. When increasing further the oxygen partial pressure, the conversion of formaldehyde, which requires more oxygen, is facilitated in the three-layer structure that offers better oxygen transfer efficiency than four-layer membranes.

As far as phenol is concerned, low pressure results were similar to those observed for formic acid and effluent A in the same conditions. However, deactivation occurs, and pressure increase lead to poor performance. This deactivation is not due to catalyst particle sintering, as cleaning-in-place procedures could recover the membrane catalytic activity. In fact, it is well known that Pt is not an adapted catalyst to run the oxidation of this molecule. Some testing with Ru-based catalytic membranes was carried out. These results showed a similar deactivation behaviour to that of the Pt-based catalytic membranes. However, this catalyst is known to require higher operating temperatures (over 150 °C), which were not accessible to our set-up.

In agreement with its content, mainly phenolic compounds (Table 3), effluent B showed a rapid deactivation. Effluent C, among other compounds, contains a complex mixture of

mineral salts, which could explain the low activity of the catalytic membrane in this case. Thanks to stronger operational conditions (Table 7), the overall performance is further improved, as required by the process development for an industrial application.

#### 4.3. Catalytic performance of multichannel systems

##### 4.3.1. Formic acid

Fig. 6 shows an increase of the reaction rate with the air overpressure for PE-4-MC. A similar effect has been observed in the case of single tubes [21]. This has been related, also in this case, to the shift of the gas–liquid interface towards the active top layer, due to the progressive liquid emptying of the porous network. According to Laplace law, at 3.6 bar the gas phase reaches the 1st intermediate layer (see Table 1). A further increase of the air overpressure does not improve significantly the reaction rate, as an overpressure of ca. 14 bars would be required to flush the liquid out from the first intermediate layer. As already observed for single tubes, the change from air to oxygen leads only to a minor increase of the reaction rate, validating diffusion rather than kinetic effect.

Fig. 6 reveals, in the case of multichannels, the same effect of the multilayer structure as that observed for single tubes. The three-layer PE-3-MC performs much better than the four-layer PE-4-MC at 3.6 bar air overpressure. This is related to the shift of the gas–liquid interface towards the active zone of PE-3-MC, as the layer supporting the catalytic top layer shows larger pore size when compared to that of PE-4-MC (0.8 and 0.2  $\mu\text{m}$ , respectively). In keeping with the similar porous structure of their intermediate layers, IN-4-MC shows a similar behaviour as PE-4-MC when increasing the gas overpressure (Fig. 6). Both present an increase of the reaction rate with the overpressure up to 3.6 bars, followed by an almost constant performance at higher pressures.

However, the catalytic performance of IN-4-MC is clearly higher. The two materials differ on various aspects: pore sizes and thickness of support and layers (Table 1), nature of catalyst support in the top layer (Table 1) and, as shown by SEM and chemical analysis (Section 3.1), catalyst distribution between channels:

- In principle, the support pore size should not affect the catalytic reaction, as this whole macroporous zone is under gas phase for the experimental conditions used here (gas overpressure above 0.5 bar). By contrast, the top layer pore size of IN-4-MC is significantly larger than that of PE-4-MC ( $\sim 80$  and  $20$  nm, respectively). As this catalytic top layer is filled up with the liquid phase, such difference in pore size may affect the transport phenomena of liquid reactants in favour of IN-4-MC. On the contrary, due to the difference in layer thickness, the distance between the gas–liquid interface and the top layer is in favor of the PE-4-MC system. It is then difficult to conclude on these morphological aspects.
- Ceria-doped zirconia-based multichannel IN membranes exhibit higher activities. This result is in good keeping with

previous results obtained on single tubes (Table 6). Ceria-doped zirconia would then be a better catalyst support than pure zirconia for this reaction, all other things being equal.

- Careful examination of the catalyst distribution among the channels, from microscopy and elemental analyses, shows a more homogeneous distribution in the case of the PE-4-MC membrane (Table 5). As a matter of fact, if the platinum loading in the external channels appears similar for both systems, this is not the case when going towards the cylindrical axis, IN-4-MC showing there a much lower catalyst loading. According to this heterogeneity, one should expect a lower performance for this membrane. However, the Pt specific surface available to the reaction, does not necessarily match the information from the above analyses. A large part of the metal surface would be out of reach of the reactant [25], as in the case of other catalytic gas–liquid systems, such as PEM fuel cells [31]. In order to check this hypothesis, membranes with much lower catalyst loading were prepared and tested. Fig. 9 shows a comparison of two very different loadings in the case of single and multichannel systems (see IN-4-ST, and IN-4-MC, normal and low loading, in Table 4).

The performance of low-loading membranes is not proportional to the very large loading difference. This demonstrates that only a limited part of the catalyst in high-loading membranes is actually active. This conclusion will have important consequences on optimising the preparation route.

#### 4.3.2. Industrial effluents

Effluent A shows a behaviour similar to what was observed on pure formic acid (Fig. 7): the effect of the three-layer structure is observed again. This trend is the same than that observed on single tubes of similar structures (Table 6). This is an interesting result from the viewpoint of up-scaling to more realistic membrane geometries and effluent composition.

Regarding effluents B and C, even if their conversion is limited, performances of the same order of magnitude are found on multichannel membranes as on single tubes.

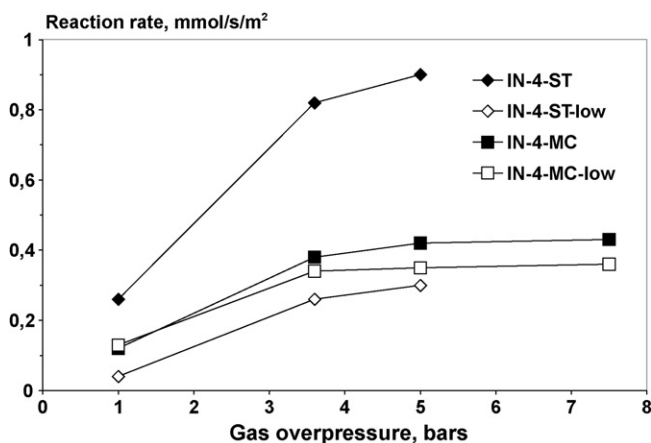


Fig. 9. Reaction rate (mmol/s/m<sup>2</sup>) as a function of gas overpressure (air) during the wet air oxidation of formic acid in an interfacial CMR at 20 °C, using different Pt loadings.

In the case of effluent B, deactivation phenomena are encountered. The complexity of this effluent makes it difficult to interpret the reasons of this deactivation. Other catalysts, such as Ru, operated at higher temperatures are under scrutiny.

For effluent C, it was observed that the low activity was not linked to the presence of salts, and moreover, that after using the membrane on this effluent, its catalytic activity for formic acid oxidation was maintained. Therefore, no deactivation could be considered here. The low overall activity may be due to the fact that only some components of the effluent can be oxidised in the present conditions.

#### 4.3.3. Techno-economical evaluation

Effluent A happens to be delivered from the chemical plant at a temperature that would allow operation of the CWAO process at 80 °C. A new technico-economical evaluation was then carried out, based on the following parameters: effluent A approximate 1100-mg<sub>TOC</sub>/l content, 3.8 mmol/s/m<sup>2</sup> reaction rate at 80 °C, 2000–2500 €/m<sup>2</sup> capital cost of membrane including platinum (less than 8% of the cost), tubing and carter. According to this approach, the investment needed per m<sup>3</sup>/h effluent treated would be of the order of 7–14,000 €/h/m<sup>3</sup>. Taking into account low operating cost, this would make the Watercattox process competitive in certain wastewater treatment applications.

## 5. Conclusions

This paper presents the progress of the WAO reaction in membrane reactors from model effluents on single tubes to real effluents on multichannel systems. A series of parameter have been identified as important towards the performance. The complexity of the catalysis in the multichannel system was shown and studied. Other process issues were considered, such as cleaning-in-place procedures.

Using commercial membrane materials that were not initially designed for this purpose, this study reached catalytic membrane performances that open the door to optimisation in membrane design, active phase nature and deposition, and operating conditions.

For this purpose, the study of this process under industrial conditions is actually under work using a pilot unit currently operated in Oslo (Norway) [23,32].

## Acknowledgements

The authors wish to express their acknowledgements to the European Commission, who funded this work through the Fifth Framework Project “Watercattox”, contract no. EVK1-CT-2000-00073. We gratefully acknowledge the assistance of Pall Exekia (France) and Inocermic GmbH (Germany) who provided the membranes supports, as well as to Monsanto Europe N.V. (Belgium) and DUE MILJOE (Norway) who supplied the industrial waste samples. The authors thank the other industrial companies and partners engaged in the Watercattox program: TREDI S.A. (France), LEK d.d. (Slovenia), MAST Carbon Ltd. (UK) and the National Institute of Chemistry of Slovenia.

## References

- [1] F.J. Zimmerman, *Chem. Eng. (N.Y.)* 25 (1958) 117.
- [2] F. Luck, *Catal. Today* 27 (1996) 195.
- [3] H. Debellefontaine, J.N. Foussard, *Waste Manage.* 20 (2000) 15.
- [4] F. Luck, *Catal. Today* 53 (1999) 81.
- [5] D. Duprez, F. Delanoe, J.J. Barbier, P. Isnard, G. Blanchard, *Catal. Today* 29 (1996) 317.
- [6] Y.I. Matatov-Meytal, M. Scheituch, *Ind. Eng. Chem. Res.* 37 (1998) 309.
- [7] S. Imamura, *Ind. Eng. Chem. Res.* 38 (1999) 1743.
- [8] J.-C. Beziat, M. Besson, P. Gallezot, S. Durecu, *J. Catal.* 182 (1999) 129.
- [9] A. Pintar, *Catal. Today* 77 (2003) 451.
- [10] F. Larachi, *Top. Catal.* 33 (2005) 109.
- [11] P. Gallezot (Ed.), *Catalytic Oxidation of Organic Waste in Water* (special issue of *Topics in Catalysis*), Springer, New York, 2005.
- [12] J. Peureux, M. Torres, H. Mozzanega, A. Giroir-Fendler, J.-A. Dalmon, *Catal. Today* 25 (1995) 409.
- [13] O.M. Ilinitch, F.P. Cuperus, L.V. Nosova, E.N. Gribov, *Catal. Today* 56 (2000) 137.
- [14] G. Centi, R. Dittmeyer, S. Perathoner, M. Reif, *Catal. Today* 79/80 (2003) 139.
- [15] R. Bredesen, H. Ræder, J.-A. Dalmon, S. Miachon, Patent EP1368278 (Europe), 2 May 2001.
- [16] R. Dittmeyer, K. Svajda, M. Reif, *Top. Catal.* 29 (2004) 3.
- [17] E.E. Iojoiu, J. Walmsley, H. Ræder, R. Bredesen, S. Miachon, J.-A. Dalmon, *Rev. Adv. Mater. Sci.* 5 (2003) 160.
- [18] S. Miachon, V. Perez, G. Crehan, E. Torp, H. Ræder, R. Bredesen, J.-A. Dalmon, *Catal. Today* (2003) 75.
- [19] H. Ræder, R. Bredesen, G. Crehan, S. Miachon, J.-A. Dalmon, A. Pintar, J. Levec, E.G. Torp, *Sep. Sci. Technol.* 32 (2003) 349.
- [20] M. Vospertnik, A. Pintar, G. Bercic, J. Levec, J. Walmsley, H. Ræder, E.E. Iojoiu, S. Miachon, J.-A. Dalmon, *Chem. Eng. Sci.* 59 (2004) 5363.
- [21] E.E. Iojoiu, J.C. Walmsley, H. Ræder, S. Miachon, J.-A. Dalmon, *Catal. Today* 104 (2005) 329.
- [22] E.E. Iojoiu, S. Miachon, J.-A. Dalmon, *Top. Catal.* 33 (2005) 135.
- [23] E.E. Iojoiu, E. Landrison, H. Ræder, E.G. Torp, S. Miachon, J.-A. Dalmon, *Catal. Today*, in press.
- [24] Watercatox project, <http://www.sintef.no/watercatox>.
- [25] G. Bercic, A. Pintar, J. Levec, *Catal. Today* 105 (2005) 589.
- [26] V. Perez, S. Miachon, J.-A. Dalmon, R. Bredesen, G. Pettersen, H. Ræder, C. Simon, *Sep. Purif. Technol.* 25 (2001) 33.
- [27] D. Uzio, S. Miachon, J.-A. Dalmon, *Catal. Today* 82 (2003) 67.
- [28] H. Ræder, R. Bredesen, E. Iojoiu, S. Miachon, J.-A. Dalmon, A. Pintar, G. Bercic, J. Levec, in: F.T. Akin, Y.S. Lin (Eds.), *Proceedings of Eighth International Conference on Inorganic Membranes*, Cincinnati, OH, USA, 18–22 July, Adams Press, Chicago, 2004, p. 394.
- [29] M. Vospertnik, A. Pintar, G. Bercic, J. Levec, *J. Membr. Sci.* 223 (2003) 157.
- [30] M. Vospertnik, A. Pintar, G. Bercic, J. Levec, *Catal. Today* 79/80 (2003) 169.
- [31] S. Miachon, Développement d'une pile à combustible hydrogène/oxygène à électrolyte polymère solide de 100 cm<sup>2</sup> à hydratation interne, PhD Thesis, University Joseph Fourier Grenoble 1, Grenoble (France), 1995, 150 pp.
- [32] Due Miljoe web site, <http://www.duemiljoe.no>.